ANL/RA/CP--85371
Conf-950420--26

Paper to be submitted for ANS Portland topical meeting (M&C) in April, 1995.

HETEROGENEOUS TREATMENT IN THE VARIATIONAL NODAL METHOD*

T. H. Fanning
University of Wisconsin—Madison, Nuclear Engineering and Engineering Physics
Madison, Wisconsin 53706

G. Palmiotti
Commissariat à l'Energie Atomique, Centre d'Etudes Nucleaires de Cadarache
SPRC BAT 230, F-13108 St. Paul-lés-Durance, France

*Work supported by the U. S. Department of Energy, Nuclear Energy Programs, under Contract W-31-109-ENG-38.

DISCLAIMER

Portions of this document may be illegible in electronic image products. Images are produced from the best available original document.

HETEROGENEOUS TREATMENT IN THE VARIATIONAL NODAL METHOD

T. H. Fanning*
University of Wisconsin—Madison
Nuclear Engineering and Engineering Physics
Madison, Wisconsin 53706
(708)252-6715

G. Palmiotti*
CEA—Cadarache
SPRC BAT 230
F-13108 St. Paul-lés-Durance
France
(708)252-2858

ABSTRACT

The variational nodal transport method is reduced to its diffusion form and generalized for the treatment of heterogeneous nodes while maintaining nodal balances. Adapting variational methods to heterogeneous nodes requires the ability to integrate over a node with discontinuous cross sections. In this work, integrals are evaluated using composite gaussian quadrature rules, which permit accurate integration while minimizing computing time.

Allowing structure within a nodal solution scheme avoids some of the necessity of cross section homogenization, and more accurately defines the intra-nodal flux shape. Ideally, any desired heterogeneity can be constructed within the node; but in reality, the finite set of basis functions limits the practical resolution to which fine detail can be defined within the node. Preliminary comparison tests show that the heterogeneous variational nodal method provides satisfactory results even if some improvements are needed for very difficult configurations.

I. INTRODUCTION

Heterogeneous treatment of reactor subassemblies could play a very important role in determining the reactivity level and power distribution of a reactor configuration. This is the case, for instance, when we want to calculate the reactivity variation due to the insertion of control rod subassemblies in fast power reactors. Commonly in design calculations, the absorber is diluted on the total surface of the subassembly—the so called "homogeneous calculation." Actually, the real "heterogeneous" description of the control rod subassembly leads to a reactivity variation that is, in general, lower (in absolute value) with respect to the homogeneous calculation.

Many methods[1–5] are available to account for the heterogeneity effect. The non-explicit ones incorporate the heterogeneity effect at the level of the cross sections, and the homogeneous description is used to calculate the reactivity. Each of these techniques rely on some type of reference calculation, where a heterogeneous cell (or supercell) description of the problem is used. Often, these methods also demand some iteration technique to find the homogeneous equivalent solution that is a priori unknown.

It is evident that an explicit description of the heterogeneity will be the best way to tackle the problem; but depending on the method adopted, a certain number of inconveniences can be encountered. Several finite difference codes need to extend the local mesh refinement to the whole reactor, increasing in an enormous way the total number of unknowns. Monte Carlo methods are very attractive due to the fact that an actual description of the heterogeneous subassembly can be made without penalizing in a significant way the calculation cost. On the other hand, heterogeneity effects are often small enough, in terms of absolute variation, to be strongly affected by the uncertainty (i.e. variance) of a non-deterministic calculation with a limited number of neutron histories.

In this paper, we propose the variational nodal method as a way to treat the explicit heterogeneous description of a subassembly. Nodal transport methods have been used increasingly in neutron transport calculations,[6] with recent

---

*Current address: Argonne National Laboratory, Reactor Analysis Division, Argonne, Illinois 60439.

advances leading to methods with near Monte Carlo accuracy at a fraction of the computing time. These are the variational nodal methods (VNM),[7–12] based on a functional for the even-parity transport equation to which odd-parity Lagrange multipliers are attached to enforce nodal balance. Response matrices are obtained by using a classical Ritz procedure in which the flux and currents are expanded in complete polynomials in space and angle.

Because of the nature of this formulation, the variational nodal method allows us to treat the cross sections as a function of the spatial variables inside the node. Therefore, an explicit description of the fine structure of the heterogeneous subassembly can be used. In this way, the heterogeneous variational nodal method (HVNM) will more accurately reproduce the intra-nodal flux shape, while obviating some of the spatial cross section homogenization that must be done.

In order to develop a methodology to treat heterogeneous nodes, the diffusion form of a functional for the even-parity transport equation is considered. It is within this framework that a two-dimensional, multigroup diffusion code has been written to examine the properties of treating heterogeneous nodes. Extending this treatment to the transport equation should be straightforward.

II. FORMULATION AND IMPLEMENTATION

A. Heterogeneous Variational Nodal Method

The response matrices used in variational nodal methods are derived from the functional for the within-group, even-parity transport equation.[7] With the problem domain spatially divided into nodes, the functional may be written as a sum over the nodal contributions. The transport functional[8] for each node includes volume and surface contributions. For node i,

$$F_i[\psi,\chi] = \int dV_i\left(\int d\hat{\Omega}\left[\frac{1}{\sigma_t}(\hat{\Omega}\cdot\nabla\psi)^2+\sigma_t\psi^2\right]-\sigma_s\varphi^2-2\varphi S\right)+2\sum_m\int d\Gamma_{im}\int d\hat{\Omega}\,(\hat{n}\cdot\hat{\Omega})\,\psi\chi\,, \tag{1}$$

where ψ and χ are the even- and odd-parity components of the angular flux and Γ_{im} represents the m^{th} surface of node i. Scattering is assumed to be isotropic, and $\int d\Omega = 1$. The remaining notation is conventional. Throughout this discussion, it is assumed that the cross sections are functions of the spatial variable r, thus allowing for inhomogeneous nodes.

It can be shown[8] that requiring Eq. (1) to be stationary with respect to variations in ψ within the node results in the even-parity transport equation. We will limit here our discussion to the diffusion approximation of the Boltzmann equation. In this case the functional becomes

$$F_i[\varphi,\hat{n}\cdot J] = \int dV_i\left[\frac{1}{3\sigma_{tr}}(\nabla\varphi)^2+\sigma_r\varphi^2-2\varphi S\right]+2\sum_m\int d\Gamma_{im}\varphi\,(\hat{n}\cdot J)\,. \tag{2}$$

The diffusion functional, Eq. (2), is first cast into algebraic form by using the classical Ritz procedure, where the unknown fluxes and currents are expanded in vectors of known functions. The fluxes and currents are then represented as a product between a vector of unknown coefficients and the vector of known functions:

$$\begin{aligned}\varphi_i(r)&\approx f^T(r)\phi_i = \phi_i^T f(r)\\ \hat{n}\cdot J_{im}(r)&\approx h^T(r)j_{im} = j_{im}^T h(r)\end{aligned} \tag{3}$$

Here, ϕ_i and j_{im} are the vectors of unknown coefficients for node i, and $f(r)$ and $h(r)$ are vectors of orthonormal basis functions that obey the orthogonality relations

$$\begin{aligned} \int dV_i f(r) f^T(r) &= V_i I \\ \int d\Gamma_{im} h(r) h^T(r) &= \Gamma_{im} I \end{aligned} \tag{4}$$

where I is the identity matrix.

Substituting Eq. (3) into Eq. (2) yields the reduced functional,

$$F_i[\phi_i, j_{im}] = \phi_i^T A_i \phi_i - 2\phi_i^T S_i + 2\sum_m \phi_i^T M_{im} j_{im} \tag{5}$$

where the matrices A_i, S_i, and M_{im} are defined as

$$\begin{aligned} A_i &= \int dV_i \left[\frac{1}{3\sigma_{tr}} \nabla f(r) \nabla f^T(r) + \sigma_i f(r) f^T(r) \right] \\ S_i &= \int dV_i f(r) S(r) \\ M_{im} &= \int d\Gamma_{im} f(r) h^T(r) \end{aligned} \tag{6}$$

In VARIANT, the current VNM code at Argonne National Laboratory,[11] all nodes must be homogeneous; and the above integrals are precalculated by factoring out the (constant) cross sections and converting the integrals to dimensionless form. But when a node is allowed to be heterogeneous, the shape, size, and distribution of the various homogeneous regions within a node are not known in advance. In order to introduce the heterogeneity treatment, each node must be broken up into a set of rectangular regions as demanded by the heterogeneous structure within the node. The result is to break up the integrals over that node into a set of homogenous integrals.

If the homogeneous regions within the heterogeneous node are defined such that

$$V_i = \sum_{l \in i} V_l, \tag{7}$$

then the integrals in Eq. (6) can be written as

$$\begin{aligned} A_i &= \sum_{l \in i} \int dV_l \left[\frac{1}{3\sigma_{tr}^l} \nabla f(r) \nabla f^T(r) + \sigma_i^l f(r) f^T(r) \right] \\ S_i &= \sum_{l \in i} \int dV_l f(r) S^l(r) \end{aligned} . \tag{8}$$

There is no change in the surface integral, as it does not depend on heterogeneous quantities.

In the reduced functional [Eq. (5)], the variation is taken with respect to the vector of unknown flux coefficients, ϕ, to arrive at the analytical approximation to the diffusion equation:

$$A_i \phi_i = S_i - \sum_m M_{im} j_{im} \tag{9}$$

Variations taken with respect to the vector of unknown current coefficients, $j_{im} = -j_{km}$, between nodes i and k, result in the flux continuity condition

$$M_{im}^T \phi_i = M_{km}^T \phi_k . \tag{10}$$

To solve Eq. (9), it is first recast into its response matrix form by defining partial current moment vectors:

$$j_{im}^{\pm} = \frac{1}{4} M_{im}^T \phi_i \pm \frac{1}{2} j_{im} \Gamma_{im}, \tag{11}$$

where j_{im}^{+} and j_{im}^{-} are the outgoing and incoming partial currents across surface m of node i. Using Eq. (11) to eliminate ϕ_i and j_{im} in Eq. (9) results in the response matrix formulation in terms of the partial currents:

$$j_i^{+} = [G_i + 2I]^{-1} B_i S_i + [G_i + 2I]^{-1} [G_i - 2I] j_i^{-}, \tag{12}$$

where $[G_i + 2I]^{-1} [G_i - 2I]$ is the response matrix for node i. The vectors $j_i^{\pm}$ are partitioned vectors containing the partial current moments for all the surfaces of node i. The matrix S_i is as before, while the matrices G_i and B_i are partitioned matrices defined as

$$\begin{aligned} [G_i]_{mm'} &= M_{im}^T A_i^{-1} M_{im'} \\ [B_i]_m &= M_{im}^T A_i^{-1} \end{aligned} \tag{13}$$

B. Implementation

A stand-alone, two-dimensional multigroup diffusion code has been written to solve the heterogeneous variational diffusion problem in Cartesian geometry. (The current VNM code used at Argonne National Laboratory, VARIANT, is limited to homogeneous nodes.) In order to allow heterogeneities in the nodal description, an efficient means of calculating the integrals of Eq. (8) must be used. To achieve this, composite gaussian quadrature rules are used.[13]

The flux expansions, in terms of the basis functions $f(r)$, are at most complete 8^{th} order polynomials in space. Since the integrals contain the term $f(r)f^T(r)$, the highest order polynomial in the integrals is 16^{th} order. Within each region, the integrals are evaluated using a ten-point gaussian quadrature rule which permits exact evaluation (within machine precision and roundoff) of up to 19^{th} order polynomials. All the integrals are precalculated and stored for later reference.

Once the integrals are in place, the initial fission source guess is made by assuming a flat flux distribution. The source matrix for node i is found by combining the standard fission and scattering source expression with Eq. (8) and Eq. (3) to arrive at

$$S_{i_g} = \sum_l \int dV_l f(r) f^T(r) \left[\sum_{g' \neq g} \sigma_{s_{g' \to g}}^l \phi_{i_{g'}}^T + \frac{\chi_g}{k} \sum_{g'} \nu \sigma_{f_{g'}}^l \phi_{i_{g'}}^T \right]. \tag{14}$$

Here, $\phi_{i_{g'}}^T$ are the flux moments from the previous source iteration. Although all the flux moments are required to evaluate the source, it is not necessary to explicitly evaluate the average flux in each homogeneous region within a heterogeneous node. Once the initial source is defined, the incoming partial currents of each node are set to zero; and the first set of inner iterations is begun.

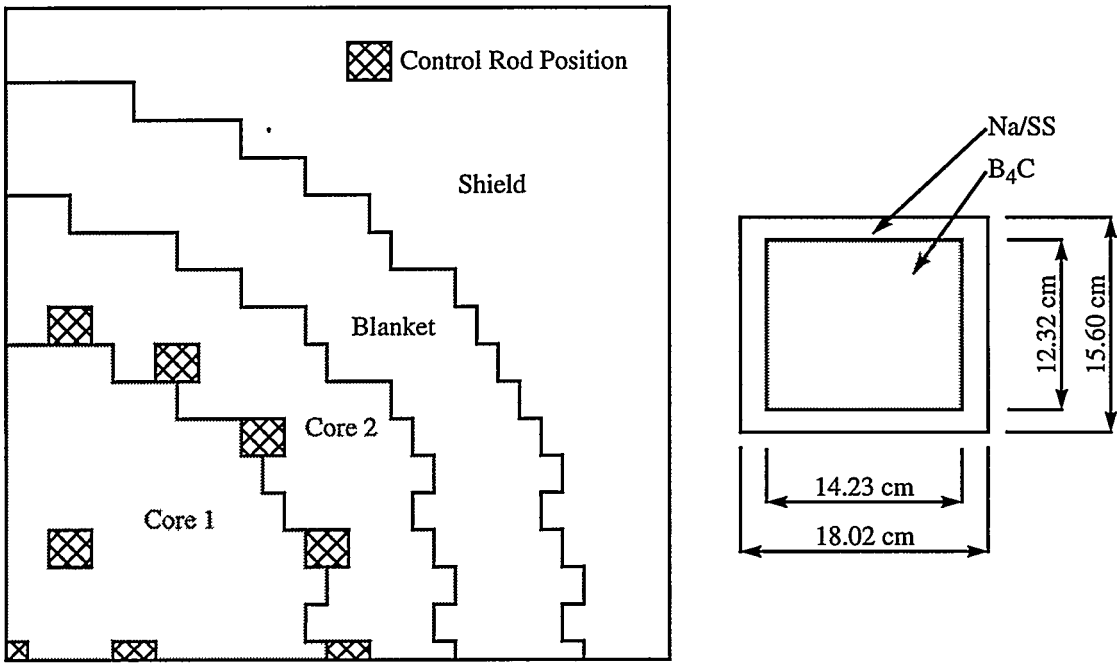

Figure 1: Core and Control Rod Models in X-Y Geometry

A red-black inner iteration scheme is used. During the first phase, the outgoing partial currents of the red nodes are calculated using Eq. (12). By combining Eq. (11) with Eq. (10), the outgoing partial currents can be used to update the incoming partial currents of the adjacent black nodes:

$$j^-_{black} = j^+_{red} \tag{15}$$

Outgoing partial currents of the black nodes are calculated in the same manner as the red nodes, and the results are used to update the incoming partial currents of the red nodes. This process is continued until all the moments of all partial currents have converged to within a specified tolerance.

When the partial currents have converged, the flux moments for each node can be determined by using Eq. (9) along with

$$j_{im} = \frac{j^+_{im} - j^-_{im}}{\Gamma_{im}}. \tag{16}$$

Using the new flux moments, an updated fission source and k are determined and checked for convergence. At present, no acceleration techniques have been employed to improve the computation time of either inner or outer iterations.

III. COMPUTATIONAL RESULTS

In order to verify the method previously presented, we consider the calculation of control rod reactivity worth of a typical large size fast reactor. The two dimensional X-Y model used is shown in Figure 1 along with the heterogeneous description of a control rod subassembly, consisting of a central strong absorber (B_4C) surrounded by a Na/SS diluted zone. A four group energy structure has been employed, and the related cross sections have been generated for

Table 1: Heterogeneity Effect for Different Configurations

Configuration	Rod Worth $\Delta\rho$ (%)[a]		Effect (%)[b]
	Heterogeneous	Homogeneous	
All Rods In	-12.174	-13.290	8.4
Center Rod In	-0.235	-0.250	6.2
First Row In	-1.106	-1.153	4.0
Second Row In	-5.057	-5.204	2.8
All In Except Half Rod in Row 2	-9.968	-10.752	7.3

[a]Reactivity variation in percent $\Delta\rho$ with respect to reference configuration where followers are present in all control rod regions.
[b]Expressed as $(\Delta\rho^{hom} - \Delta\rho^{het}) / \Delta\rho^{hom}$.

all compositions, including the homogeneous control rod where the standard design approximation of volume weighted densities has been applied.

In Table 1, the results obtained for the heterogeneity effect (in terms of percent variation of reactivity with respect to the reference configuration, where a sodium follower is present in all the control rod zones) are shown for different configurations of control rod insertions. Very large effects (more than 8%) can be observed for some configurations. Actually, because these calculations have been performed using diffusion theory, those effects are generally underestimated, while transport calculations would have provided larger values. We can also observe that the heterogeneity effects are space dependent. Depending on the position of the inserted control rod in the core, the heterogeneity effect can be strongly different. The main reason for this is related to the different flux gradients at the positions of the control rods.

In Table 2, reactivity variations are compared between the reference solution using the explicit representation of the heterogeneity within a refined mesh and HVNM, where only one node is used but the cross section spatial dependence is taken into account to describe the heterogeneity. Note that in the reference solution, because a refined mesh is used, the increase in number of nodes per subassembly is propagated to all subassemblies lying in the same band, leading to a total number of nodes over two times greater than the standard meshing.

Results are shown for different approximations of the surface and intra-node variables. We can observe that little is gained increasing the order of the expansion on the surface of the node. On the contrary, the accuracy is improved by going to higher order polynomials inside the node. We recall that, currently in VARIANT, only up to fourth order expansion is allowed within the node for Cartesian geometries. The comparison looks quite satisfactory, except perhaps, the configuration with all control rods inserted where, even using an eighth order expansion, a 2% error was found with respect to the reference solution.

In order to better understand the difficulty of the problem, we can look to Figure 2 where the total flux traverse along the x axis is plotted for different solutions in the case of all control rods inserted. A zoom to the "half" control rod of the first ring shows that the reference flux is very difficult to be reproduced by an eighth order polynomial expansion. Moreover, the flux gradient is discontinuous where material changes inside the node occur. HVNM shows a smooth flux because only one basis of polynomials is used over the entire node. In any case, the HVNM solution presents a large improvement with respect to the homogeneous representation.

Table 3 shows the computational time required by the various solutions. As can be seen in the table, the addition of the heterogeneity treatment used by HVNM imposes virtually no penalty to the computational effort as compared

Table 2: Comparison of Control Rod Worth between an Explicit Description and the HVNM Code

Polynomial Order		Reference	HVNM			
	Surface	2	1			2
	Volume	6	4	6	8	6
Rod Worth (%)[a] (% error[b])	All Rods In	-12.174	-12.694 (4.3)	-12.527 (2.9)	-12.445 (2.2)	-12.539 (3.0)
	Center Rod In	-0.235	-0.240 (2.4)	-0.239 (1.7)	-0.238 (1.3)	-0.239 (1.8)
	First Row In	-1.106	-1.129 (2.1)	-1.122 (1.4)	-1.118 (1.1)	-1.123 (1.5)
	Second Row In	-5.057	-5.137 (1.6)	-5.111 (1.1)	-5.099 (0.8)	-5.114 (1.1)
	All In Except Half Rod in Row 2	-9.968	-10.350 (3.8)	-10.227 (2.6)	-10.166 (2.0)	-10.235 (2.7)

[a]Reactivity variation in percent $\Delta\rho$ with respect to reference configuration where followers are present in all control rod regions.
[b]Calculated as $(\Delta\rho^{HVNM} - \Delta\rho^{Reference}) / \Delta\rho^{Reference}$.

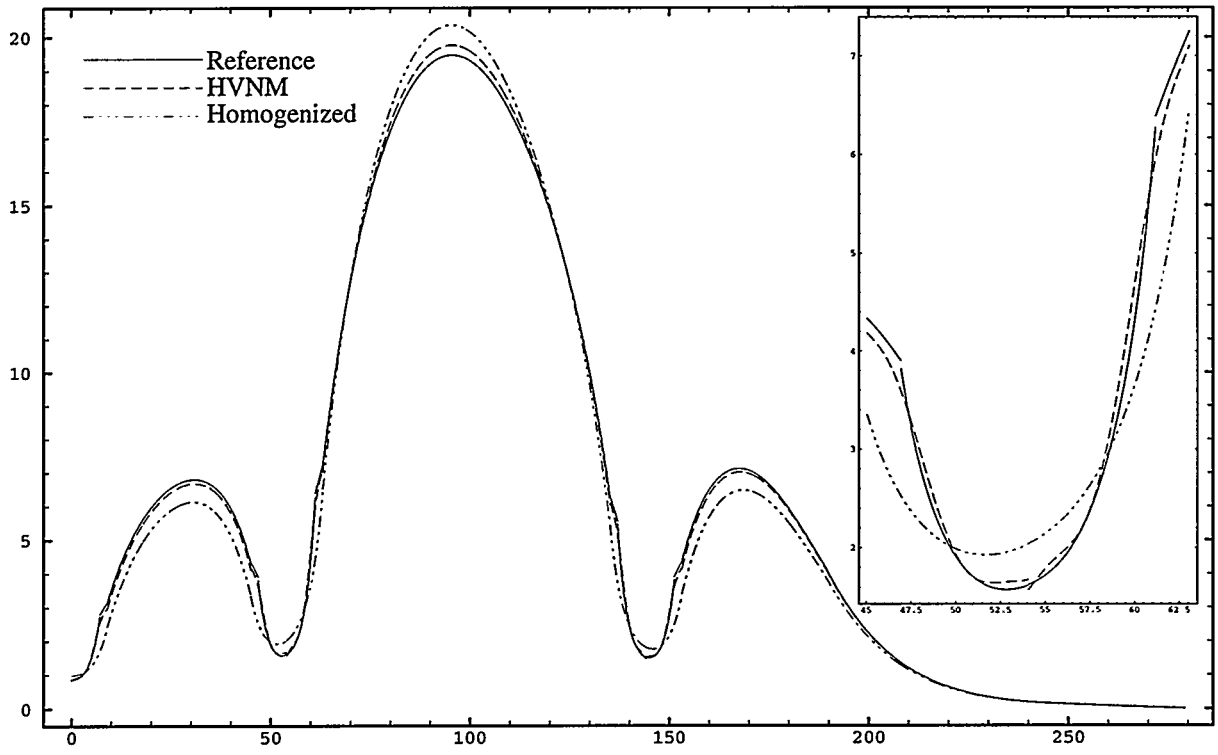

Figure 2: Total Flux Along x Axis (Inset Shows Flux in Half Rod of Row 1)

Table 3: Timing results for the Various Solution Methods

Configuration	Total Time by Solution Type[a] (sec)		
	Reference	Homogeneous	HVNM
All Rods In	1960	940	873
Center Rod In	766	314	317
First Ring In	909	379	387
Second Ring In	1660	690	717
All In Except Half Rod in Ring 1	3240	1390	1413

[a]Times are shown for sixth order internal expansions and linear surface expansions.

to the standard homogeneous treatment. The reference solution, on the other hand, requires twice as much time due to the increase in number of nodes.

At present, the HVNM code enforces the same order of internal approximation for all the nodes. An obvious improvement will be to have selected nodes (in particular, the ones we want to treat heterogeneously) with different, more accurate expansion orders (up to 10 or 12). The iteration scheme and total number of surface unknowns will not change because the expansion order on the node surface will be kept the same (linear) everywhere. This option will allow improved results without penalizing the computation time in a significant way. Most of the nodes (i.e. the homogeneous ones) will keep the standard fourth order internal approximation. Other possible improvements might employ the use of a different basis of functions or the possibility to deal with piecewise functions inside the node.

IV. CONCLUSIONS

Because of its formulation, the variational nodal method is well suited to be employed in the explicit description of the fine structure of heterogeneous nodes. We have presented the formulation modification with respect to the original method to take into account the spatial dependence of cross sections inside a node. The HVNM method has been implemented in a two-dimensional Cartesian code using multigroup diffusion theory.

Calculational comparisons have shown quite satisfactory results even if some improvements are needed for very difficult configurations. For this purpose, in the future, the code will be extended to allow different orders of internal approximations by node. Transport theory will also be implemented in order to provide more realistic results.

In addition, different geometries, including curvilinear ones like circles inside subassemblies, have to be treated to better represent the real fine structure of heterogeneous subassemblies. Finally, in the case where a continuous basis of functions inside the node will not be accurate enough to represent the shape of the intra-nodal flux, the use of piecewise polynomials may be necessary.

ACKNOWLEDGMENTS

The authors would like to acknowledge C. Carrico of Argonne National Laboratory for his invaluable assistance in keeping up to date with the constantly evolving variational nodal methods. This work was done in part at Argonne National Laboratory under the support of a laboratory graduate fellowship program.

REFERENCES

1. J. L. Rowlands and C. R. Eaton, "The Spatial Averaging of Cross-Sections for Use in Transport Theory Reactor Calculations, with an Application to Control Rod Fine Homogenization," *Proc. Specialists' Mtg. Homogenization Methods in Reactor Physics*, Lugano, Switzerland, November 13–15, 1978.

2. T. Takeda et al., *Ann. Nucl. Energy*, **8**, 509 (1982).

3. M. Carta, G. Granget, G. Palmiotti, M. Salvatores, and R. Soule, "Control Rod heterogeneity Effects in Liquid-Metal Fast Breeder Reactors: Method Developments and Experimental Validation," *Nuclear Science and Engineering*, **100**, pp. 269–276 (1988).

4. K. S. Smith, "Assembly Homogenization Techniques for Light Water Reactor Analysis," *Progress in Nuclear Energy*, Vol. 17, No. 3, pp. 303–335 (1986).

5. A. Trkov and M. Ravnik, "Effective Diffusion Homogenization of Cross Sections for Pressurized Water Reactor Core Calculations," *Nuclear Science and Engineering*, **116**, pp. 86–95 (1994).

6. A. Badruzzaman, "Nodal Methods in Transport Theory," *Advances in Nuclear Science and Technology*, Vol. 21, J. Lewins and M. Becker, Eds., Plenum Press, New York, New York (1990).

7. E. E. Lewis and W. F. Miller, *Computational Methods of Neutron Transport*, Chap. 6, John Wiley & Sons, New York, New York (1984).

8. I. Dilber and E. E. Lewis, "Variational Nodal Methods for Neutron Transport," *Nuclear Science and Engineering*, **91**, pp. 132–142 (1985).

9. E. E. Lewis, "Interface Angular Coupling Reductions in Variational Nodal Methods for Neutron Transport," *Nuclear Science and Engineering*, **102**, pp. 140–152 (1989).

10. C. B. Carrico, E. E. Lewis, and G. Palmiotti, "Three-Dimensional Variational Nodal Transport Methods for Cartesian, Triangular, and Hexagonal Criticality Calculations," *Nuclear Science and Engineering*, **111**, pp. 168–179 (1992).

11. G. Palmiotti, C. B. Carrico, and E. E. Lewis, "Variational Nodal Transport Methods with Anisotropic Scattering," *Nuclear Science and Engineering*, **115**, pp. 233–243 (1993).

12. J. M. Ruggieri, R. Boyer, F. Malvagi, and J. Y. Doriath, "Local Mesh Refinement in Reactor Calculation Using Variational Nodal Method," *Proceedings of the International Conference on Reactor Physics and Reactor Computations*, Tel-Aviv, January 23–26, 1994, pp. 617–624 (1994).

13. S. D. Conte and Carl de Boor, *Elementary Numerical Analysis, An Algorithmic Approach*, Third Edition, pp. 311–327, McGraw-Hill, Inc., New York, New York (1980).